JACC: CARDIOVASCULAR INTERVENTIONS
© 2016 BY THE AMERICAN COLLEGE OF CARDIOLOGY FOUNDATION
PUBLISHED BY ELSEVIER

VOL. 9, NO. 5, 2016
ISSN 1936-8798/$36.00
http://dx.doi.org/10.1016/j.jcin.2016.01.008

Novel 3-Dimensional Vessel and Scaffold Reconstruction Methodology for the Assessment of Strut-Level Wall Shear Stress After Deployment of Bioresorbable Vascular Scaffolds From the ABSORB III Imaging Substudy

Bill D. Gogas, MD, PhD,[a,b] Boyi Yang, PhD,[b,c] Marina Piccinelli, PhD,[b,d] Don P. Giddens, PhD,[b,e]
Spencer B. King III, MD,[a,b,f] Dean J. Kereiakes, MD,[g] Stephen G. Ellis, MD,[h] Gregg W. Stone, MD,[i]
Alessandro Veneziani, PhD,[b,c] Habib Samady, MD[a,b]

A 72-year-old female patient underwent successful deployment of a single 3.0 × 18 mm Absorb bioresorbable vascular scaffold (Abbott Vascular, Santa Clara, California) to the mid right coronary artery (**Figures 1A and 1B**). The scaffolded segment was imaged simultaneously with coronary angiography and with the C7 Dragonfly (LightLab Imaging Inc., St. Jude Medical, Westford, Massachusetts) optical coherence tomographic (OCT) system at 100 frames/s with a motorized pull-back speed of 20 mm/s and a flush rate of 3 ml/s. Images demonstrated adequate scaffold apposition, with no evidence of edge dissections or tissue prolapse (**Figure 1C**).

This patient was enrolled in the ongoing imaging substudy of the ABSORB III randomized clinical trial, RESTORATION (Evaluation and Comparison of Three-Dimensional Wall Shear Stress Patterns and Neointimal Healing Following Percutaneous Coronary Intervention with the Absorb Everolimus-Eluting Bioresorbable Vascular Scaffold Compared to the Xience V Everolimus-Eluting Metallic Stent), which aims to evaluate the differential effects of the Absorb bioresorbable vascular scaffold compared with the Xience metallic stent on local hemodynamic conditions at 3 years (1). The OCT study endpoints include the changes in wall shear stress (WSS) from post-procedure to 3-year follow-up and the relationship between strut-level derived WSS after deployment to neointimal tissue healing at 3 years.

The fusion of 3-dimensional angiographic acquisitions (including vessel curvature) with OCT imaging (**Figures 1A to 1C**) is a novel approach for the assessment of vessel-level and strut-level WSS following device deployment. This novel methodological approach includes the following steps: 1) semiautomatic strut detection from the OCT image acquisition through shape recognition algorithms; 2) semiautomatic reconstruction of the scaffold wire frame that displays the patient-specific scaffold pattern; 3) automatic lumen extraction following stacking of the OCT cross sections over the patient-specific vessel curvature obtained from angiography; 4) realignment of the stent wire frame to the patient-

---

From the [a]Andreas Gruentzig Cardiovascular Center, Division of Cardiology, Department of Medicine; [b]Emory Cardiovascular Imaging & Biomechanics Core Laboratory, Emory University School of Medicine, Atlanta, Georgia; [c]Department of Mathematics and Computer Science; [d]Department of Radiology and Imaging Sciences; [e]Wallace H. Coulter Department of Biomedical Engineering, Georgia Institute of Technology and Emory University, Atlanta, Georgia; [f]Saint Joseph's Heart and Vascular Institute, Atlanta, Georgia; [g]Christ Hospital Heart and Vascular Center and The Carl and Edyth Lindner Center for Research and Education at The Christ Hospital, Cincinnati, Ohio; [h]Cleveland Clinic Foundation, Cleveland, Ohio; and the [i]Columbia University Medical Center, New York Presbyterian Hospital, and The Cardiovascular Research Foundation, New York, New York. Abbott Vascular is the sole sponsor of the ABSORB III randomized clinical trial. The authors have reported that they have no relationships relevant to the contents of this paper to disclose.

Manuscript received December 23, 2015; revised manuscript received January 5, 2016, accepted January 6, 2016.

FIGURE 1 In Vivo Assessment of Computational Fluid Dynamics Derived From Fusion of Optical Coherence Tomographic and Angiographic Acquisitions Following Deployment of a Bioresorbable Vascular Scaffold

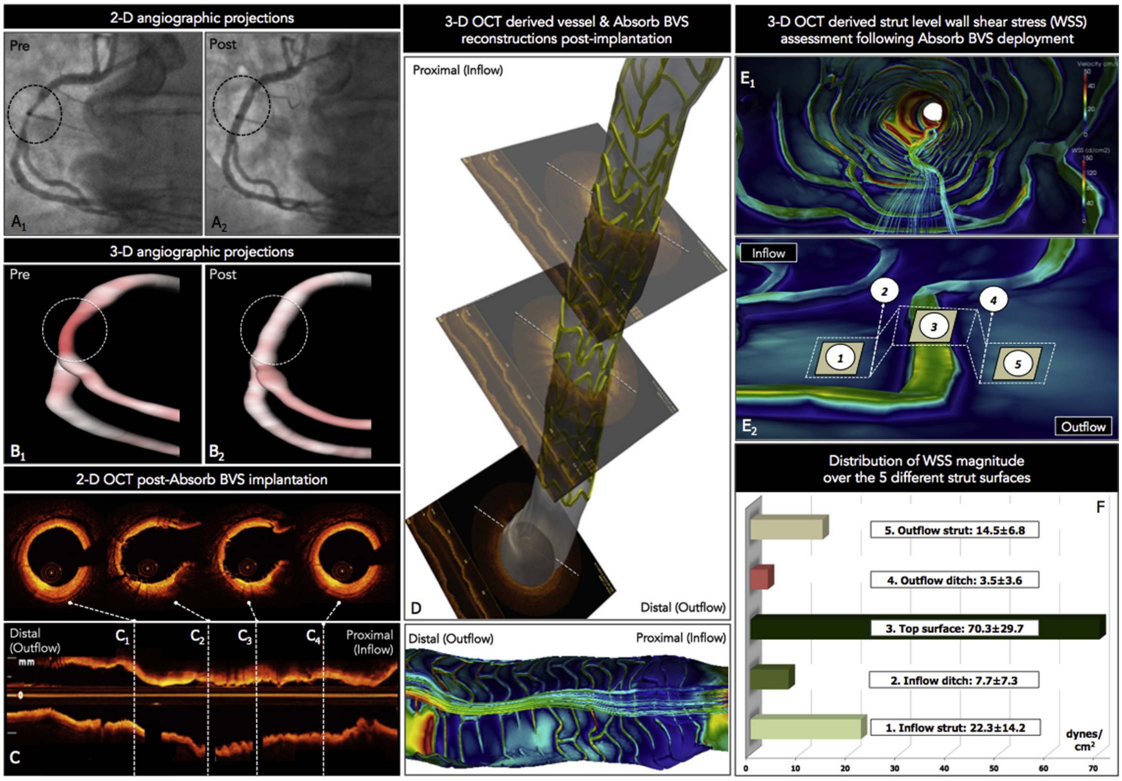

(A1,A2,B1,B2) Two-dimensional (2-D) single-plane angiographic projections demonstrating the significant mid right coronary artery (RCA) lesion as well as the treated mid-RCA segment with a bioresorbable vascular scaffold (BVS). Three-dimensional (3-D) anatomies are generated by fusing 2-dimensional angiographic projections with angle difference of at least 45°. **(C)** Two-dimensional longitudinal (L-view) optical coherence tomographic (OCT) view of the scaffolded segment with selected cross sections from the distal (outflow), scaffolded, and proximal (inflow) segments. **(C_2,C_3)** Optimally deployed scaffold with a small intimal tear at 1 o'clock **(C_3)**. **(D)** Lumen and scaffold reconstructions following stacking of the segmented optical coherence tomographic cross sections bended over the patient-specific angiographic anatomy. **(E1,E2)** Numeric modeling of the reconstructed 3-dimensional computational fluid dynamics domain visualizing velocity streamlines and wall shear stress (WSS) magnitude in the scaffolded segment as well as the proximal and distal edge segments. WSS magnitude is calculated in 5 different surfaces: the inflow strut, the inflow ditch, the top of the strut, the outflow ditch and the outflow strut. **(F)** Bar graph demonstrating the distribution of WSS magnitude over the 5 different strut surfaces. Average WSS was lowest at the outflow ditch (3.5 dynes/cm^2) and highest at the top strut surface (70.3 dynes/cm^2).

specific curvature and reconstruction of the stent geometry onto the wireframe (**Figure 1D**); 5) subtraction of the scaffold strut geometry to obtain the computational fluid dynamics domain; 6) prescription of realistic boundary conditions; and 7) computational fluid dynamics analysis using finite element methods over the reconstructed domain (**Figures $1E_1$ and $1E_2$**).

We will prospectively investigate whether the larger struts of bioresorbable scaffolds (strut thickness ≈ 150 μm) will generate greater microcirculatory zones of low WSS at the strut sides (**Figure $1E_2$**, strut surfaces 2 and 4) compared with the metallic stents (strut thickness 81 μm) (2,3). We postulate that the resultant robust neointimal generation in response to the low WSS, in conjunction with the ongoing resorption of the struts, will result in a homogenous neointimal response that will reduce the risk for late or very late scaffold thrombosis (4) (**Figures $1E_2$ and 1F**).

ACKNOWLEDGMENT Dr. Yang wishes to acknowledge the Emory Laney Graduate School.

REPRINT REQUESTS AND CORRESPONDENCE: Dr. Habib Samady, Emory University School of Medicine, 1364 Clifton Road, Suite F606, Atlanta, Georgia 30322. E-mail: hsamady@emory.edu.

REFERENCES

1. Kereiakes DJ, Ellis SG, Popma JJ, et al. Evaluation of a fully bioresorbable vascular scaffold in patients with coronary artery disease: design of and rationale for the ABSORB III randomized trial. Am Heart J 2015;170:641–51.

2. Ellis SG, Kereiakes DJ, Metzger DC, et al. Everolimus-eluting bioresorbable scaffolds for coronary artery disease. N Engl J Med 2015;373:1905–15.

3. Gogas BD, King SB III, Timmins LH, et al. Biomechanical assessment of fully bioresorbable devices. J Am Coll Cardiol Intv 2013;6:760–1.

4. Stone GW, Granada JF. Very late thrombosis after bioresorbable scaffolds: cause for concern? J Am Coll Cardiol 2015;66:1915–7.

KEY WORDS bioresorbable scaffolds, optical coherence tomography, patient-specific computational fluid dynamics